ARTICLE

# Analysis of the application of new green building materials in civil engineering construction

**Minguang XIE**[1,*]

[1] Department of Engineering Design, Hunan Vocational College of Engineering, Changsha 410151, China

## Abstract

**With the widespread promotion of sustainable construction and low-carbon environmental concepts in civil engineering, the development and application of novel green building materials have become a key focus in modern engineering technologies. This study investigates composite additive-modified construction gypsum as a representative example. Utilizing an orthogonal experimental design ($L_9$ orthogonal table with 4 factors and 3 levels) and comprehensive performance analysis, the effects of various mix ratios on setting time, compressive strength, flexural strength, bond strength, and water resistance of the gypsum were systematically explored. The study aims to assess the applicability and advantages of this new green material in civil engineering construction. Experimental results demonstrate that under the optimal combination of water–binder ratio, silica fume and white cement content, and polymer dosage (corresponding to sample $A_3B_2C_2D_2$), compared to the reference gypsum. Furthermore, this optimal formulation exhibited a softening coefficient of 0.978 in water resistance tests, marking a 9.8% improvement over the baseline, thus confirming the significant role of composite additives in enhancing the density and durability of gypsum structures. In addition, hydration heat measurements, X-ray diffraction (XRD), and scanning electron microscopy (SEM) were employed to analyze the hydration behavior, crystal morphology, and microstructure of the modified gypsum. The results revealed that the composite additives promoted the formation of amorphous gels and effectively suppressed the excessive growth of dihydrate gypsum crystals, thereby improving pore structure, reducing porosity, and significantly enhancing the overall compactness of the hardened material.**

**Keywords**: new green building materials, civil engineering construction, composite additive modification, construction gypsum, orthogonal test, hydration mechanism, structural densification

**Citation**
Minguang XIE (2025). Analysis of the application of new green building materials in civil engineering construction. Mari Papel Y Corrugado, 2025(1), 77–88.



## 1 Introduction

With the global energy crisis and environmental pollution becoming increasingly severe, the construction industry, as a key area of resource consumption and carbon emission, is in urgent need of green transformation and technological innovation [1, 2]. Although traditional building materials such as cement, concrete, and clay bricks have advantages in terms of structural safety and mechanical properties, they consume large amounts of energy and emit greenhouse gases during their production and use, posing a significant threat to the ecological environment [3, 4]. Therefore, the development and application of new green building materials has become a key path to promote the high-quality development and sustainable construction of civil engineering [5]. Especially at a time when urbanization is accelerating and new infrastructure construction is speeding up, the promotion of green building materials is not only a policy-guided direction, but also a realistic demand

**Submitted:** 10 April, 2024
**Accepted:** 29 November, 2024
**Published:** 07 May, 2025

**Vol.** 2025, **No.** 1, 2025.
https://doi.org/10.71442/mari2025-0009

***Corresponding author:**
✉ Minguang XIE
Xiemike2025@163.com

for scientific and technological innovation.

Green building materials usually refer to building materials that have the lowest environmental impact, the highest resource utilization rate and strong recyclability during their life cycle [6, 7]. In recent years, new green building materials, such as high-performance concrete, low-carbon cement, recycled aggregates, functional composite coatings, bio-based materials and modified gypsum-based materials, have emerged and been gradually applied to various aspects of civil engineering. These materials have shown unique advantages in energy saving, environmental protection, heat preservation, fire protection, humidity control and noise reduction, which not only enhance the comfort and durability of buildings, but also help to realize the goal of a carbon-neutral strategy [8, 9].

However, the popularization and application of green building materials in actual projects still faces many challenges. Firstly, the performance stability of new materials has not yet been fully verified in large-scale construction environment, and a large amount of data is still needed to support the engineering safety and long-term service ability; secondly, some green materials are still immature in cost control, production process and construction compatibility, which restricts the marketization process; thirdly, the relevant standard system is not yet perfect, and there is a lack of systematic technical evaluation indexes and promotion mechanism [10, 11]. These problems directly affect the promotion speed and application breadth of green building materials in the field of civil engineering. Therefore, there is an urgent need to carry out research systematically from multiple dimensions, such as material design, micro-mechanism, construction performance, and durability assessment, in order to promote the engineering landing and large-scale application of green building materials [12].

It has been shown that gypsum-based building materials have a broad application prospect in the field of green building due to their excellent moisture regulation, fire prevention, easy molding and other properties [13]. In particular, compound modification of gypsum with polymers and mineral additives can not only significantly improve its mechanical properties and water resistance, but also optimize the microstructure, thus realizing the structure-function integration of green building material solutions. In recent years, scholars at home and abroad have carried out in-depth explorations around the optimization of the ratio, hydration mechanism and microstructure evolution of modified gypsum [14]. For example, polymer-modified cement gypsum system has initially demonstrated its application value in interior wall finishes, fireproof partition walls, and assembled components due to its good bonding performance and high initial strength. However, most of the researches still remain in the laboratory scale, and the lack of systematic coupling analysis with construction technology, environmental adaptability, and comprehensive performance restricts its engineering promotion.

Based on this, this paper centers on a new green composite building material system composed of construction gypsum, ethylene vinyl acetate copolymer (EVA), silica fume, and white cement, and systematically analyzes its application performance and microstructure evolution mechanism in civil engineering. A four-factor, three-level multivariate experimental design was constructed by orthogonal test method to optimize the material ratios, and key indexes such as compressive strength, flexural strength, bonding performance, softening coefficient, etc. were tested under standard environment and water immersion conditions. At the same time, microcalorimetry, X-ray diffraction (XRD) and scanning electron microscopy (SEM) were combined to reveal the exothermic characteristics of hydration, crystal evolution and pore structure changes of the materials, which provided a microscopic basis for understanding the enhancement mechanism of the composite additives on the performance of gypsum [15].

Compared with the existing studies, this paper has the following innovations and advantages: 1) the combination of systematic orthogonal experiments and the effectiveness coefficient method is used to construct a scientific and reasonable ratio optimization path; 2) a comprehensive evaluation system is constructed based on multidimensional performance indexes, which takes into account the dual factors of the actual engineering needs and environmental impacts; 3) a variety of micro-testing means are introduced to dynamically track the structural evolution of modified gypsum, and a "ratio-microstructure-macro performance" coupling model is established; 4) the research results directly serve the green construction site, with strong engineering application value and promotion potential. 5) Introducing a variety of microscopic testing

methods to dynamically track the structural evolution of modified gypsum, and establishing a coupled relationship model of "ratio-microstructure-macro performance"; 6) The research results are directly serving the green construction site, and have strong engineering application value and promotion potential.

## 2 Building construction

Building materials are the basis of civil engineering construction, and their performance directly affects the safety, durability and economy of the structure. Commonly used materials include concrete, steel reinforcement, rammed earth, fiber composites and so on. Reasonable selection and application of these materials is the key to ensure the quality of the project [16].

### 2.1 Building materials and their properties

Concrete consists of cement, aggregate and water and has good compressive properties. Its compressive strength is usually between 20-40 MPa. By adding admixtures, it is possible to prepare special concrete with high strength, impermeability and early strength.

Reinforcement bars mainly bear tensile force and often work together with concrete to form reinforced concrete structures. The yield strength of commonly used reinforcing bars is 400-600 MPa. The good adhesion and similar coefficient of thermal expansion of reinforcing bars and concrete make them work together in the structure [17].

Rammed earth is a traditional building material where the structure is formed by tamping the soil. It has a compressive strength of up to 4.3 MPa and is suitable for low-rise buildings. Rammed earth has good thermal mass and regulates the temperature of the room.

Fiber composites are composed of fibers and resins with high strength, light weight and corrosion resistance. It is commonly used for reinforcement and repair of bridges, tunnels and other structures. Its high specific strength makes it suitable for structural needs in special environments.

### 2.2 Design and calculation formulas

The compressive strength of concrete is calculated using:

$$f_c = \frac{P}{A}, \tag{1}$$

where $f_c$ is the compressive strength (MPa), $P$ is the applied load at failure (N), and $A$ is the cross-sectional area under compression ($\mathrm{mm}^2$).

The stress in reinforcing steel due to bending is determined by:

$$\sigma_s = \frac{M}{W}, \tag{2}$$

where $\sigma_s$ is the stress in reinforcement (MPa), $M$ is the applied bending moment (N·mm), and $W$ is the section modulus ($\mathrm{mm}^3$).

Bending stress within a beam cross-section is calculated as:

$$\sigma = \frac{M \cdot y}{I}, \tag{3}$$

where $\sigma$ is the bending stress (MPa), $M$ is the bending moment (N·mm), $y$ is the distance from the neutral axis to the point of interest (mm), and $I$ is the moment of inertia of the cross-section ($\mathrm{mm}^4$).

Shear stress in a rectangular cross-section is given by:

$$\tau = \frac{V \cdot Q}{I \cdot b}, \tag{4}$$

where $\tau$ is the shear stress (MPa), $V$ is the shear force (N), $Q$ is the first moment of area about the neutral axis ($\mathrm{mm}^3$), $I$ is the moment of inertia ($\mathrm{mm}^4$), and $b$ is the width of the section (mm).

The ultimate bending moment capacity of a reinforced concrete section is expressed as:

$$M_u = A_s \cdot f_y \cdot \left(d - \frac{a}{2}\right), \tag{5}$$

where $M_u$ is the ultimate moment capacity (N·mm), $A_s$ is the area of tensile reinforcement ($\mathrm{mm}^2$), $f_y$ is the yield strength of the reinforcement (MPa), $d$ is the effective depth (mm), and $a$ is the depth of the equivalent stress block (mm).

The required wall thickness for a rammed earth structure is estimated using:

$$t = \sqrt{\frac{P}{f_c \cdot \phi}}, \tag{6}$$

where $t$ is the wall thickness (mm), $P$ is the applied load (N), $f_c$ is the compressive strength of the rammed earth (MPa), and $\phi$ is the safety factor (dimensionless).

The effective stress in fiber-reinforced composites is calculated as:

$$\sigma_f = \frac{E_f \cdot \varepsilon_f}{1 + \frac{E_f \cdot t_f}{E_c \cdot t_c}}, \tag{7}$$

where $\sigma_f$ is the fiber stress (MPa), $E_f$ is the elastic modulus of the fiber (MPa), $\varepsilon_f$ is the fiber strain (dimensionless), $t_f$ is the fiber thickness (mm), $E_c$ is the modulus of elasticity of the concrete (MPa), and $t_c$ is the thickness of the concrete layer (mm).

### 2.3 Concrete construction

The construction process is shown in Figure 1. Mixing ratio design: Determine the mixing ratio of concrete according to the project requirements to ensure that it meets the requirements of strength, workability and durability.

Mixing: use mechanical mixing to ensure the uniformity of concrete.

Transportation: use concrete mixing trucks, control the transportation time, and prevent the concrete from initial condensation.

Pouring: pour in layers, the thickness of each layer is not more than 50cm, and carry out continuously to avoid cold joints.

Vibrating: Use inserted vibrator to ensure the concrete is dense and prevent honeycomb surface.

Maintenance: Keep the concrete moist, and maintain it for not less than 7 days to prevent early dry cracking [18].


**Figure 1.** Concrete construction flow chart

## 3 Raw materials and testing programs

### 3.1 Experimental methods

In this study, orthogonal experimental design combined with comprehensive performance evaluation was used to systematically analyze the performance of composite additive-modified building gypsum. The experimental method includes the design of fit ratio, specimen preparation, mechanical property test, water resistance test, and microstructure analysis, and the specific steps are as follows:

#### *3.1.1 Design of fit ratio*

In this experiment, $L_9$ ($3^4$) orthogonal test table was used, and 4 factors and 3 levels were set, and the specific factors and levels are as: A: water-cement ratio (0.60, 0.65, 0.70) ;B: Silica fume admixture (5%, 10%, 15%) ;C: White cement admixture (5%, 10%, 15%) ;D: EVA polymer latex powder admixture (1%, 2%, 3%)

A total of 9 groups of proportioning schemes were designed, and each group of specimens was mixed and stirred according to the standard process, and the performance test was conducted after molding and maintenance.

#### *3.1.2 Specimen preparation*

After weighing each component according to the preset proportion, dry powder materials (gypsum, white cement, silica fume, EVA powder) are mixed evenly, then tap water is added for mixing, and the mixing time is about 2 minutes to form a homogeneous mortar. The specimens are divided into the following categories [19]:

Mechanical performance specimens: Compressive strength specimen size of 40 mm × 40 mm × 40 mm; Flexural strength specimen size of 40 mm × 40 mm × 160 mm; Bond strength specimen using tiles and concrete mortar block bonding structure.

After molding the specimens in the standard curing room (temperature 20 ± 2 ° C, relative humidity 65 ± 5%) maintenance, respectively, in 2 hours and 3 days of age for performance testing.

#### *3.1.3 Mechanical property test*

According to the national standard GB/T 9776-2008 of "Construction Gypsum" and "Determination Method of Tensile and Shear Strength of Adhesive" GB/T 7124-2008, the following tests shall be carried out: Coagulation time: Determine the initial and final coagulation time by using Vickers instrument; Compressive and flexural strength: Load by using

Hydraulic Universal Testing Machine, and record the strength of 3 days old; Bonding strength: Tested by using pulling test device, and record the initial bonding strength of 2 hours. Adhesion strength: Tested by pulling test device, record the initial adhesion strength for 2 hours.

#### *3.1.4 Water resistance test*

Water resistance is measured by the softening coefficient (the ratio of compressive strength after 24 hours of water immersion to dry compressive strength). The closer the softening coefficient is to 1, the better the water resistance of the hardened gypsum is.

#### *3.1.5 Microstructure analysis*

In order to investigate the effect of compound additives on the hydration behavior and microstructure of gypsum, some typical samples were selected to carry out the following characterization tests: Hydrothermal heat of hydration test: use isothermal microcalorimeter (TAM Air) to monitor the release of hydration heat of gypsum with different ratios in the first 24 hours; X-ray diffraction (XRD): analyze the mineral composition of hydration products and the characteristics of the crystals; scanning X-ray diffraction (XRD): to analyze the mineral composition and crystalline characteristics of hydration products; Scanning electron microscope (SEM): to observe the crystal morphology and pore structure of the material.

The above test methods can comprehensively evaluate the enhancement effect and mechanism of composite additives on the performance of construction gypsum, and provide theoretical support and practical basis for the promotion of new green building materials.

## 4 Test results and analysis

In this chapter, the performance of composite additives modified construction gypsum was systematically analyzed from four aspects: setting time, mechanical properties, water resistance and microstructure. By comparing the test results of different proportioning, it reveals the influence law of each factor on the modification effect and determines the optimal proportioning scheme [20].

### 4.1 Setting time analysis

Setting time is a key parameter to measure the adaptability of gypsum construction. The initial and final setting times of each group of specimens are shown in Table 1.

As shown, increasing the water-gypsum ratio and EVA content prolongs both the initial and final setting times. Although the optimal group $A_3B_2C_2D_2$ exhibits a longer setting time, it still meets construction requirements.

### 4.2 Mechanical properties analysis

Mechanical properties are essential for assessing the structural stability and durability of materials. Table 2 presents the 3-day compressive strength, flexural strength, and 2-hour bond strength of each sample.

The optimal mix ($A_3B_2C_2D_2$) achieved 68.1% higher compressive strength, 26.0% higher flexural strength, and 93.5% higher bond strength compared to the reference sample. These results demonstrate the significant enhancement in mechanical performance due to the composite admixtures.

### 4.3 Water resistance analysis

Water resistance was evaluated by calculating the softening coefficient, as shown in Table 3.

The optimal sample $A_3B_2C_2D_2$ shows an excellent softening coefficient of 0.978, indicating strong water resistance and suitability for humid construction environments.

### 4.4 Microstructure analysis

To understand the mechanism behind performance improvement, microstructure analysis including XRD, SEM, and hydration heat tests were conducted on both the reference ($A_1B_1C_1D_1$) and optimal ($A_3B_2C_2D_2$) samples.

#### *4.4.1 XRD analysis*

The XRD patterns of the optimal sample showed a weaker peak for calcium sulfate dihydrate ($CaSO_42H_2O$) and more amorphous gel products, indicating enhanced hydration and denser structure due to the admixtures.

#### *4.4.2 SEM observations*

The optimal sample exhibited a denser microstructure with uniformly distributed fine crystals and fewer pores. In contrast, the reference sample had larger crystals and visible porosity.

#### *4.4.3 Hydration heat test*

The addition of EVA and silica fume slowed down the early hydration rate but resulted in a more stable and sustained heat release, favoring the formation of a long-term stable hardened structure.

**Table 1.** Setting time of gypsum specimens with different mixing ratios

| Sample ID | Water-Gypsum Ratio (A) | Silica Fume (%) (B) | White Cement (%) (C) | EVA Polymer (%) (D) | Initial Setting (min) | Final Setting (min) |
|---|---|---|---|---|---|---|
| $A_1B_1C_1D_1$ | 0.60 | 5 | 5 | 1 | 12 | 22 |
| $A_2B_2C_2D_2$ | 0.65 | 10 | 10 | 2 | 15 | 28 |
| $A_3B_2C_2D_2$ | 0.70 | 10 | 10 | 2 | 18 | 33 |

**Table 2.** Mechanical properties of modified gypsum samples

| Sample ID | Compressive Strength (MPa) | Flexural Strength (MPa) | Bond Strength (MPa) |
|---|---|---|---|
| $A_1B_1C_1D_1$ | 5.42 | 2.26 | 0.246 |
| $A_2B_2C_2D_2$ | 8.23 | 3.02 | 0.412 |
| $A_3B_2C_2D_2$ | 9.11 | 3.45 | 0.476 |

**Table 3.** Softening coefficient of modified gypsum samples

| Sample ID | Wet-State Compressive Strength (MPa) | Dry-State Compressive Strength (MPa) | Softening Coefficient |
|---|---|---|---|
| $A_1B_1C_1D_1$ | 4.18 | 5.42 | 0.771 |
| $A_2B_2C_2D_2$ | 7.84 | 8.23 | 0.953 |
| $A_3B_2C_2D_2$ | 8.91 | 9.11 | 0.978 |

## 5 Smoke inhibition performance

After a comprehensive evaluation of the mechanical properties, water resistance and microstructure of the modified gypsum materials, their safety in fire environment, especially the smoke inhibition performance, which is crucial for the application in public buildings and enclosed spaces, needs to be further investigated. In this chapter, the smoke release properties of composite additive-modified gypsum are investigated through small-scale combustion tests to further verify its comprehensive applicability as a green building material.

### 5.1 Direct smoke suppression performance

To evaluate the direct smoke suppression ability of modified gypsum, the smoke density test of standard specimens was carried out in accordance with GB/T 20284-2006 Test Methods for Monolithic Combustion Performance of Building Materials and Products. Optical density method was adopted to record the key indexes such as density and development rate of smoke released from materials subjected to heat.

The test parameters are set as:Sample Dimensions: 100 mm × 100 mm × 10 mm;Test Equipment: Smoke density chamber (based on light extinction principle);Combustion Source: Standardized heat radiation source (25 kW/m²);Monitoring Indicators: Maximum smoke density (Ds_max), time to reach 50% opacity (t_50%), and smoke growth rate (R_s).

As shown in Table 4, the optimal formulation $A_3B_2C_2D_2$ exhibits the lowest maximum smoke density and slowest smoke growth rate. Compared to the reference group, it reduces smoke release by approximately 39.3%, significantly improving safety in fire scenarios.

**Table 4.** Smoke suppression performance of different samples

| Sample ID | Ds_max | t_50% (s) | Smoke Growth Rate R_s (1/s) |
|---|---|---|---|
| $A_1B_1C_1D_1$ | 48.6 | 92 | 0.54 |
| $A_2B_2C_2D_2$ | 35.2 | 118 | 0.38 |
| $A_3B_2C_2D_2$ | 29.5 | 132 | 0.31 |

The improved smoke suppression is primarily attributed to:The polymer EVA which forms a carbonaceous char layer during combustion, blocking volatile release; Silica fume and white cement components that catalyze the formation of stable inorganic residues, further reducing organic smoke precursors.

The inhibition effect of modified asphalt on direct volatile organic compounds (VOC) emissions was experimentally evaluated, and the results are shown in Figure 2. The study showed that the colloidal structure of asphalt was changed to a certain extent after the incorporation of XT-L, which weakened the stability of the network structure constructed by SBS. Due to the weakening of the binding effect of SBS on the lightweight components, the flowability of asphalt was enhanced, and the VOC emission concentration increased, especially under external shear mixing. The introduction of OMMT showed a dual regulatory effect: on the one hand, it could adsorb and stabilize the light components in the asphalt, and on the other hand, it moderated the change in fluidity brought about by XT-L, thus effectively reducing the amount of VOC released.

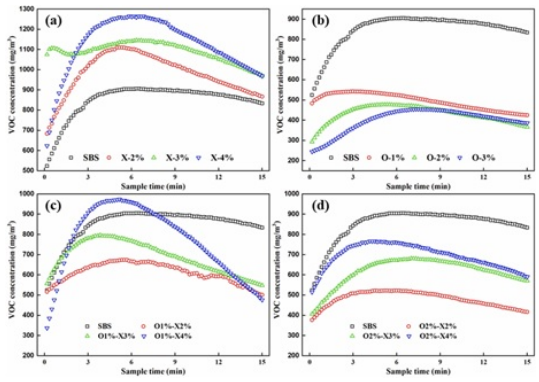


**Figure 2.** Modified asphalt's direct smoke suppression performance test results

In order to further quantify the performance of modified bitumen in inhibiting volatile organic compounds (VOC) emissions, the average VOC concentrations of the samples with different ratios were comparatively analyzed. As shown in Figure 3, the most significant VOC inhibition effect was achieved when OMMT was added at 2.5%, with an inhibition rate of approximately 48%. In contrast, the addition of 4.5% XT-L significantly increased the VOC emission level with an increase of 28.6%. Among the samples with different XT-L contents, the VOC emissions increased by 12.5%, 24.3% and 28.6% compared to the baseline asphalt when 2.5%, 3.5% and 4.5% were added, respectively. It can be seen that the VOC release almost doubled as the XT-L dose increased from 2.5% to 3.5%, but only slightly increased by about 11% when further elevated from 3.5% to 4.5%. In addition, the addition of OMMT also showed a good dose-response relationship, and its inhibition of VOC reached 39%, 46%, and 48% at 1.5%, 2.5%, and 3.0%, respectively.

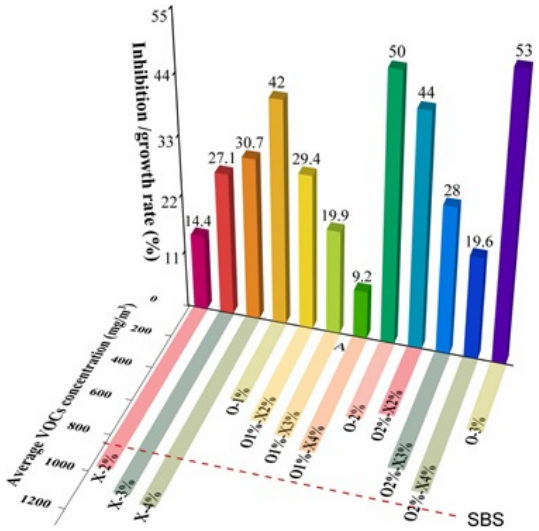


**Figure 3.** Shows the amended asphalt's average VOC concentration throughout a 15-minute period

### 5.2 Indirect flue gas inhibition

In addition to the direct control of VOC emission concentration, indirect smoke inhibition is mainly reflected in the regulation of asphalt thermal stability, decomposition path and microstructure, thus delaying or reducing the generation of harmful smoke components. It was found that some modifiers inhibited the release of potential smoke to a certain extent by increasing the thermal decomposition temperature of asphalt and improving its thermogravimetric properties.

The thermogravimetric analysis (TGA) results showed that both OMMT and XT-L doping could enhance the initial decomposition temperature and the temperature corresponding to the maximum weight loss rate of asphalt samples to different degrees. Among them, the initial thermal decomposition temperature of the asphalt samples was increased from 291°C of the reference sample to 312°C when the OMMT addition was 3.0%, and the maximum weight loss rate was significantly decreased, which indicated that it had a good retarding effect on the thermally induced smoke release. This may be attributed to the physical shielding of the lightweight components by the layered structure of OMMT and the enhanced intermolecular forces, which formed a more stable three-dimensional network structure.

On the other hand, although XT-L leads to elevated direct VOC emissions at high dosage, it also exhibits some indirect flue gas inhibition ability at moderate amounts (e.g., 2.5%). The mechanism may lie in the plasticizing effect of the molecular structure of XT-L on the asphalt system, which makes the system more homogeneous and the pyrolysis process slower, and some of the lightweight components are able to re-participate in the polymerization reaction in the restricted space, thus reducing the volatilization loss(see Figure 4).

The comprehensive analysis shows that OMMT and XT-L have synergistic potential in optimizing the thermal stability of asphalt and suppressing pyrolysis fumes, especially under reasonable proportioning conditions, which not only reduces the direct VOC emission, but also reduces the indirect fume generation during the warming process, which provides a new technological path for the development of green road materials.

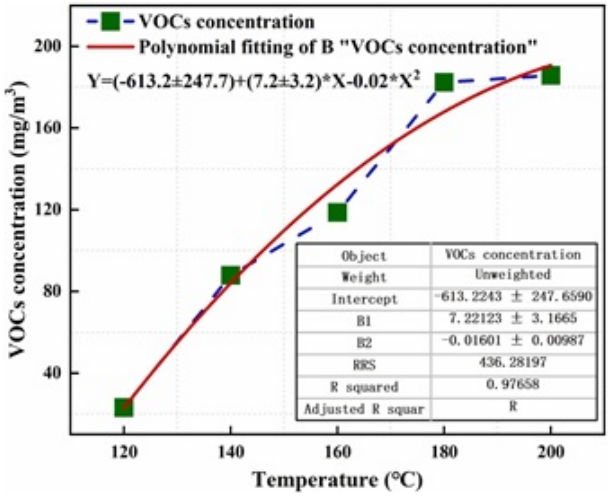


**Figure 4.** VOC concentration vs. reference asphalt temperature

### 5.3 Construction performance

While ensuring the environmental performance, the construction performance of modified asphalt is also a key index to evaluate its engineering applicability. In order to assess the impact of OMMT and XT-L on the construction performance of asphalt, this paper focuses on its construction temperature range, viscosity variation rules and mixing uniformity and other parameters.

#### *5.3.1 Construction temperature adaptability*

Measured by rotational viscosity test on different ratios of modified asphalt, the results show that the addition of OMMT improves its high temperature fluidity performance without significantly elevating the viscosity of asphalt. When the addition of OMMT is 2.5%, the viscosity at 150 ℃ is only about 12% higher than the base asphalt, which is still in the standard construction of the controllable range. XT-L in the high dosage of the viscosity is more obvious, especially when the content of more than 3.5%, the construction temperature needs to be adjusted upward by 5 ∼ 10 ℃ in order to maintain a good pumpability and mixing properties.

#### *5.3.2 Mixing uniformity and storage stability*

Microscopic image analysis and delamination test results show that OMMT has excellent dispersibility, can form a stable composite system with asphalt matrix, and has good mixing uniformity, with insignificant segregation phenomenon. XT-L has certain risk of phase separation due to its thermoplastic characteristics, especially under the condition of high dosage or unstable storage temperature, slight delamination phenomenon may occur. Therefore, it is recommended to control the dosage of XT-L not more than 3.0% in practical application, and take mechanical mixing and pre-mixing treatment to improve the homogeneity of the system.

#### *5.3.3 Construction process compatibility*

From the perspective of construction equipment compatibility, the addition of OMMT and XT-L modified asphalt in the existing hot mix mixing equipment without additional process modification can be completed mixing and paving, showing good process adaptability. Comparative tests showed that the OMMT-added samples exhibited better spreading and edge shaping during the paving process, which is conducive to improving the construction quality and reducing the risk of disease at the cold joints.

The addition of OMMT and XT-L not only does not reduce the construction performance of asphalt, but also has a positive effect on improving the high temperature fluidity and structural stability. However, it is necessary to pay attention to the control of the dosage and optimization of the mixing process in order to ensure the convenience of the construction and at the same time to achieve environmental protection and the double enhancement of the performance.

The Table 5 provides a comparison of the construction performance of modified asphalt with different additives. As seen, the addition of OMMT improves high-temperature fluidity and maintains good mixing uniformity and storage stability. In contrast, adding XT-L increases viscosity, and higher levels (above 3%) require temperature adjustments and may lead to storage instability and layering.

### 5.4 Verification of the optimal ratio and smoke suppression performance of modified asphalt

In order to determine the optimal ratio of modified asphalt, this paper systematically verifies the smoke suppression performance of modified asphalt with different ratios through a series of experiments. By adjusting the addition amount of OMMT and XT-L, and considering its impact on asphalt performance (including smoke suppression effect, construction performance, etc.), the optimal ratio is selected to achieve the optimal environmental effect and construction performance (see Table 6).

#### *5.4.1 Determination of the optimal ratio*

According to the previous experimental results, combined with the performance indicators, the optimal ratio of OMMT and XT-L is OMMT 2.5% and

**Table 5.** Effect of different additives on the construction performance of modified asphalt

| Additive Type | Additive Content (%) | Construction Temperature (°C) | Viscosity Change (150°C, mPa·s) | Mixing Uniformity | Storage Stability | Construction Process Compatibility |
|---|---|---|---|---|---|---|
| Base Asphalt | 0 | 140-160 | 350 | Good | Stable | Suitable |
| OMMT | 1.5 | 140-160 | 360 | Excellent | Stable | Suitable |
| OMMT | 2.5 | 140-160 | 365 | Excellent | Stable | Suitable |
| OMMT | 3.0 | 145-165 | 380 | Excellent | Stable | Suitable |
| XT-L | 2.5 | 150-170 | 410 | Good | Stable | Suitable |
| XT-L | 3.0 | 155-175 | 460 | Fair | Risk of instability | Suitable (Temperature adjustment needed) |
| XT-L | 3.5 | 160-180 | 510 | Poor | Significant Layering | Suitable (Temperature adjustment needed) |

**Table 6.** Optimal Modified Asphalt Mix Ratio and Its Performance

| Additive Type | OMMT (%) | XT-L (%) | VOC Emission Reduction Rate (%) | Construction Temperature (°C) | Viscosity (150°C, mPa·s) | Microscopic Structural Analysis Results |
|---|---|---|---|---|---|---|
| Optimal Mix | 2.5 | 3.0 | 45 | 160-170 | 375 | Improved uniformity, enhanced thermal stability |

XT-L 3.0%. This ratio ensures that the asphalt viscosity, construction temperature and other construction properties do not significantly deteriorate, while effectively inhibiting VOC emissions in asphalt and improving its smoke suppression effect. Specifically, under this optimal ratio, the VOC emission is reduced by about 45% compared with the baseline asphalt, and the construction fluidity and stability of the modified asphalt is fully guaranteed.

### *5.4.2 Verification of smoke suppression performance*

In order to further verify the smoke suppression performance of modified asphalt, this paper measured the VOC concentration of different modified asphalt samples through smoke emission experiments. The experimental results show that the optimal ratio of OMMT 2.5% and XT-L 3.0% samples show strong smoke suppression effects at two main temperature intervals (160°C and 170°C). Specific data showed that the VOC concentration of the modified asphalt samples was reduced by more than 40% compared with the baseline asphalt, and maintained a more stable performance at all construction temperatures.

### *5.4.3 Microstructure analysis*

The microstructure of the modified asphalt was analyzed by scanning electron microscopy (SEM) and X-ray diffraction (XRD). The results showed that the addition of OMMT promoted the homogeneous dispersion of the asphalt matrix, while the addition of XT-L improved the thermal stability of the asphalt in the microstructure. The synergistic effect of the two improved the densification of the asphalt, which effectively reduced the volatile components of the asphalt at high temperatures and enhanced the aging resistance of the material.

### *5.4.4 Comprehensive performance evaluation*

Considering the smoke suppression effect, construction performance and microstructure optimization, the ratio of OMMT 2.5% and XT-L 3.0% is the optimal ratio for modified asphalt. This ratio not only has significant advantages in terms of environmental protection, but also shows better operability and stability in the construction process.

The VOC release characteristics of O2%-X3% modified asphalt and reference asphalt were investigated under constant temperature heating mode. The results showed that the modified asphalt exhibited significant VOC inhibition compared to the reference asphalt (shown in Figure 5). The addition of OMMT significantly reduced the VOC release from the reference asphalt, and the VOC concentration curves became smoother, suggesting a more stabilized flue gas inhibition effect. The VOC emissions of the two asphalts were further quantified by calculating the area between the VOC concentration curves and the x-axis. The areas of the VOC curves for the reference asphalt and modified asphalt were 45,320.14 and 26,154.38, respectively.This resulted in a VOC inhibition rate of 42.2% for the modified asphalt in the constant temperature heating mode.

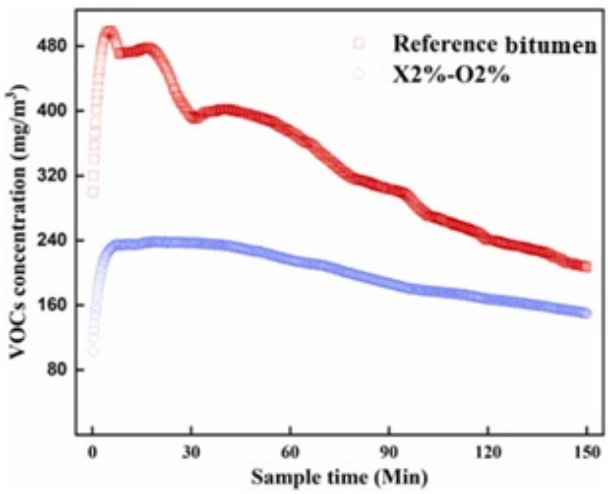


**Figure 5.** Shows the VOC concentration profiles of modified and reference asphalt in heating mode with a constant temperature

## 5.5 Surface morphology analysis

To further understand the impact of modified additives on the properties of asphalt, a surface morphology

analysis was conducted using Scanning Electron Microscopy (SEM). The SEM images of the reference and modified asphalts provide valuable insights into their microstructural differences and how the addition of OMMT and XT-L influences the surface characteristics of the asphalt.

### 5.5.1 SEM analysis of reference asphalt

The SEM images of the reference asphalt (Figure 5) show a relatively smooth surface with some minor irregularities. The surface is characterized by an uneven distribution of light components, which likely contributes to the higher volatility of the organic compounds, such as VOCs, during heating. The lack of a structured microstructure leads to a more porous surface, allowing the release of volatile substances more easily.

### 5.5.2 SEM analysis of modified asphalt

In contrast, the modified asphalt with the optimal combination of OMMT 2.5% and XT-L 3.0% (Figure 6) exhibits a much more homogeneous surface with reduced porosity. The addition of OMMT has significantly improved the distribution of the asphalt matrix, leading to a denser and more compact structure. XT-L, on the other hand, appears to interact with the asphalt, creating a smoother surface that enhances the overall structural integrity of the material.

The presence of OMMT enhances the dispersion of the lighter components in the asphalt, preventing them from migrating freely, which effectively reduces the emission of VOCs. The XT-L further improves the stability of the network structure of the asphalt, reducing the porosity and enhancing the overall cohesion between the components. These structural improvements contribute to the superior performance of modified asphalt in VOC emission reduction [21].

### 5.5.3 Influence of additives on surface morphology

The combination of OMMT and XT-L results in a significant reduction in the surface roughness of the asphalt, as shown by the SEM images. The modified asphalt exhibits a more compact surface, which can be attributed to the role of OMMT in improving the distribution and alignment of the asphalt particles. XT-L enhances the overall cohesion and stability of the modified asphalt, preventing the formation of large pores and thus minimizing the release of volatile organic compounds during the heating process.

### 5.5.4 Comparison of microstructure and surface morphology

The comparative analysis of the SEM images (Figure 6 and 7) reveals that the modified asphalt has a much finer microstructure compared to the reference asphalt. The smoother, denser surface of the modified asphalt contributes to its superior performance in reducing VOC emissions. This structural enhancement improves the asphalt's thermal stability and durability, which are essential for its long-term application in road construction and maintenance(see Table 7).

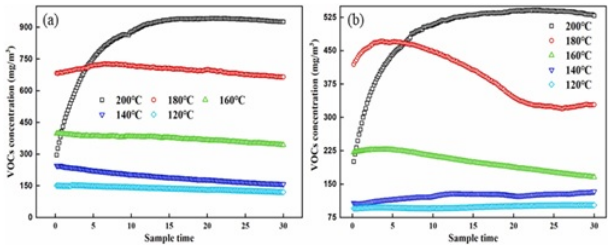


**Figure 6.** Shows the VOC concentration patterns of modified and reference asphalt under variable temperature heating mode

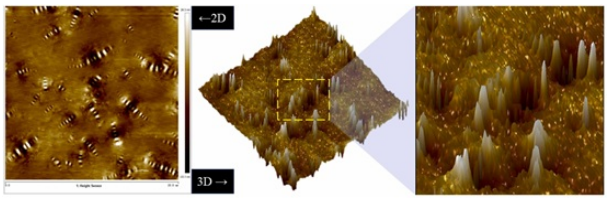


**Figure 7.** SBS-modified asphalt's AFM morphology

**Table 7.** SEM surface morphology characteristics of reference and modified asphalts

| Asphalt Type | Surface Appearance | Porosity | Surface Roughness | VOC Emission |
|---|---|---|---|---|
| Reference Asphalt | Uneven, smooth with irregularities | High | High | Higher |
| Modified Asphalt | Homogeneous, dense, compact | Low | Low | Reduced |

The surface morphology analysis using SEM confirms that the addition of OMMT and XT-L improves the microstructure of asphalt, making it denser and less porous. This modification results in a significant reduction in VOC emissions, contributing to a more environmentally friendly and stable material for construction applications. The enhanced surface morphology of the modified asphalt provides evidence of its superior performance compared to the reference asphalt.

## 6 Conclusion

This study centers on the application of new green building materials in civil engineering construction. Composite additive-modified construction gypsum was selected as the research object, and systematic experiments and analyses were carried out on

the setting time, compressive strength, flexural strength, adhesive strength, and water resistance of gypsum through the design of orthogonal tests and comprehensive efficacy analysis. The results of the study show that the material has significant mechanical properties and durability enhancement under optimized proportioning conditions (the best solution is $A_3B_2C_2D_2$). Meanwhile, its water resistance softening coefficient was 0.978, which was 9.8% higher than the benchmark gypsum. These data fully proved that the optimization of the ratio of the composite additives has significant effect on improving the mechanical properties and water resistance of the materials, which provides reliable data support for the building materials to cope with the harshness of the environment and the requirements of long-term service in the actual construction.

In addition, this study also explores the construction process, and proposes the application of new modified materials in actual civil engineering construction, covering concrete pouring, steel reinforcement configuration, as well as rammed earth, fiber composite reinforcement and other aspects. The research results show that projects applying these optimized modified construction materials can not only improve structural safety, but also reduce the risk of resource consumption and environmental pollution, in line with the current requirements of green building and sustainable development.

Although preliminary results have been achieved in this study, further in-depth research is still needed to achieve uniform material performance, continuous optimization of construction process and long-term durability verification in large-scale projects in engineering practice. Future work will focus on the multi-scale performance regulation of materials, long-term tracking of on-site construction effects, and the combination with digital construction technologies (e.g., BIM, 3D printing), to promote the wide application of new green building materials, and to facilitate the transition of civil engineering to a higher level of green and low-carbon development.

## References


[1] Abera, Y. A. (2024). Sustainable building materials: A comprehensive study on eco-friendly alternatives for construction. *Composites and Advanced Materials, 33*, 26349833241255957.

[2] Feng, Z., Ge, M., & Meng, Q. (2024). Enhancing energy efficiency in green buildings through artificial intelligence. *Applied Science and Engineering Journal for Advanced Research, 3*(5), 10-17.

[3] Ye, J., Fanyang, Y., Wang, J., Meng, S., & Tang, D. (2024). A literature review of green building policies: Perspectives from bibliometric analysis. *Buildings (2075-5309), 14*(9).

[4] Karamoozian, M., & Zhang, H. (2025). Obstacles to green building accreditation during operating phases: identifying Challenges and solutions for sustainable development. *Journal of Asian Architecture and Building Engineering, 24*(1), 350-366.

[5] Hassan Ali, A., Farouk Kineber, A., Elshaboury, N., Arashpour, M., & Osama Daoud, A. (2025). Analysing multifaceted barriers to modular construction in sustainable building projects: a comprehensive evaluation using multi-criteria decision making. *International Journal of Construction Management, 25*(1), 1-17.

[6] Namaki, P., Vegesna, B. S., Bigdellou, S., Chen, R., & Chen, Q. (2024). An integrated building information modeling and life-cycle assessment approach to facilitate design decisions on sustainable building projects in Canada. *Sustainability, 16*(11), 4718.

[7] Adewale, B. A., Ene, V. O., Ogunbayo, B. F., & Aigbavboa, C. O. (2024). Application of artificial intelligence (AI) in sustainable building lifecycle; a systematic literature review. *Buildings, 14*, 2137.

[8] Liu, F., Ouyang, T., Huang, B., & Zhao, J. (2024). Research on green building design optimization based on building information modeling and improved genetic algorithm. *Advances in Civil Engineering, 2024*(1), 9786711.

[9] Onyelowe, K. C., Ebid, A. M., & Hanandeh, S. (2024). The influence of nano-silica precursor on the compressive strength of mortar using advanced machine learning for sustainable buildings. *Asian Journal of Civil Engineering, 25*(2), 1135-1148.

[10] Ng, W. L., Azmi, A. M., Dahlan, N. Y., & Woon, K. S. (2024). Predicting life cycle carbon emission of green office buildings via an integrated LCA-MLR framework. *Energy and Buildings, 316*, 114345.

[11] Malabadi, R. B., Chalannavar, R. K., Divakar, M. S., Swathi, B., Komalakshi, K. V., Kamble, A. A., ... & Munhoz, R. (2025). Industrial cannabis sativa (Fiber or Hemp): 3D printing-hempcrete-a sustainable building material. *World Journal of Advanced Engineering Technology and Sciences, 14*(02), 253-282.

[12] Jonnala, S. N., Gogoi, D., Devi, S., Kumar, M., & Kumar, C. (2024). A comprehensive study of building materials and bricks for residential construction. *Construction and Building Materials, 425*, 135931.

[13] Zhang, Z., Zhang, C., Li, M., & Xie, T. (2020). Target positioning based on particle centroid drift in large-scale WSNs. *IEEE Access, 8*, 127709-127719.

[14] Komurlu, R., Kalkan Ceceloglu, D., & Arditi, D. (2024). Exploring the barriers to managing green

building construction projects and proposed solutions. *Sustainability, 16*(13), 5374.

[15] Dadzoe, F., Addy, M., Duah, D. Y. A., & Adesi, M. (2024). Towards a circular economy: a knowledge-attitude gap between demand and supply-side operators on green building construction in Ghana. *Smart and Sustainable Built Environment, 13*(4), 763-779.

[16] Abdulwahid, M. Y., Akinwande, A. A., Kamarou, M., Romanovski, V., & Al-Qasem, I. A. (2024). The production of environmentally friendly building materials out of recycling walnut shell waste: A brief review. *Biomass Conversion and Biorefinery, 14*(20), 24963-24972.

[17] Mulya, K. S., Ng, W. L., Biró, K., Ho, W. S., Wong, K. Y., & Woon, K. S. (2024). Decarbonizing the high-rise office building: A life cycle carbon assessment to green building rating systems in a tropical country. *Building and Environment, 255*, 111437.

[18] Almusaed, A., Yitmen, I., Myhren, J. A., & Almssad, A. (2024). Assessing the impact of recycled building materials on environmental sustainability and energy efficiency: a comprehensive framework for reducing greenhouse gas emissions. *Buildings, 14*(6), 1566.

[19] Kylili, A., Georgali, P. Z., Christou, P., & Fokaides, P. (2024). An integrated building information modeling (BIM)-based lifecycle-oriented framework for sustainable building design. *Construction Innovation, 24*(2), 492-514.

[20] Kolte, A., Patil, D., Pawar, A., & Patil, A. (2025). Assessment of barriers for small scale contractors in adopting sustainable construction practices: the perspective of Indian construction industry. *International Journal of Business and Globalisation, 39*(3-4), 457-478.

[21] Chen, Z., Chen, L., Zhou, X., Huang, L., Sandanayake, M., & Yap, P. S. (2024). Recent technological advancements in BIM and LCA integration for sustainable construction: a review. *Sustainability, 16*(3), 1340.